# Multiplexing radiography using a carbon nanotube based x-ray source

J. Zhang
*Department of Radiation Oncology, University of North Carolina, Chapel Hill, North Carolina 27599*

G. Yang
*Department of Physics and Astronomy, University of North Carolina, Chapel Hill, North Carolina 27599*

Y. Z. Lee
*School of Medicine, University of North Carolina, Chapel Hill, North Carolina 27599*

S. Chang
*Department of Radiation Oncology, University of North Carolina, Chapel Hill, North Carolina 27599*

J. P. Lu and O. Zhou[a)]
*Department of Physics and Astronomy, University of North Carolina, Chapel Hill, North Carolina 27599 and Curriculum in Applied and Materials Sciences, University of North Carolina, Chapel Hill, North Carolina 27599*

(Received 3 April 2006; accepted 26 May 2006; published online 9 August 2006)

Speed and temporal resolution are critical for tomographic imaging of objects in rapid motion. Current x-ray scanners record images *sequentially* in the time domain. The serial approach limits their performance and demands increasingly high x-ray peak power and gantry speed. We have developed a multipixel carbon nanotube based field emission x-ray source that produces spatially and temporally modulated radiations. Using this device we show the feasibility of *multiplexing* radiography that enables *simultaneous* collection of multiple projection images using frequency multiplexing. A drastic increase of the speed and reduction of the x-ray peak power are achieved without compromising the imaging quality. © *2006 American Institute of Physics*.
[DOI: 10.1063/1.2234744]

Computed tomography[1,2] (CT) has found wide acceptance in fields such as clinical diagnosis,[3] industrial inspection, and security screening. Limited-angle tomographic methods have also been developed for detection of breast cancer[4] and for inspection of microelectronics.[5] Recently micro-CT has emerged as a powerful *in vivo* imaging tool for preclinical cancer studies in small animals.[6,7] In all CT systems a large number of projection images from a wide viewing angle ranges are required for reconstruction. As a result a fast scanning speed is essential to image objects in rapid motion such as for diagnosis of cardiovascular diseases,[8] CT fluoroscopy,[9] and airport luggage inspection. The current CT scanners collect the projection images *sequentially* in the time domain, by a step-and-shoot process using a single-pixel x-ray source. The inefficient *serial* data collection scheme demands an increasingly high x-ray peak power and gantry rotation speed, both of which have approached the physical limits.[10,11]

The imaging speed can in principle be significantly increased by multiplexing,[12] as demonstrated in communication devices and in certain analytical instruments.[13,14] Multiplexing, however, has not been applied to x-ray radiography, partly due to limitations of the x-ray source technology. Conventional x-ray tubes are single-pixel devices that generate radiation from one focal point ("pixel") on the x-ray anode. As a result mechanical motion of either the source or the object is required to obtain the different views, as illustrated in Fig. 1(a) (left). The radiation wave form can not be readily programed which makes coding and decoding difficult. These limitations can be mitigated by the multipixel field emission x-ray technology we recently reported.[15,16] This multipixel x-ray source, using the carbon nanotubes[17] (CNTs) as the field emission cathode, can generate a plurality of spatially distributed x-ray beams (pixels) with programmable intensity, pulse width, and repetition rate.[18] This spatially distributed x-ray source technology opens the door for system configurations such as *stationary* CT scanners that record the multiple views without mechanical motion of the gantry[15] and multiplexing tomographic imaging, both of which have the potential to significantly increase the CT imaging speed.

The experiment was carried out using the orthogonal frequency division multiplexing (OFDM) algorithm[19] in a configuration illustrated in Fig. 1(a) (right). The x-ray source comprised a linear array of nine CNT electron field emission cathodes, a shared common gate, electrostatic focusing optics, and a molybdenum target housed in $10^{-8}$ Torr vacuum. To ensure uniform emission across the pixels a rheostat ($R_D$) was put in series with each cathode, which also functioned as a ballast resistor to minimize the current fluctuation.[20] The gate voltage $V_g$ and the rheostat were calibrated to achieve the desired current and thus x-ray flux from each pixel. The voltage of the electrostatic focusing electrode $V_f$ was adjusted for each pixel[21] to obtain a uniform 200 $\mu$m focal spot size for all nine pixels. During operation the anode voltage $V_a$ was fixed at 40 kV and $V_g$ was adjusted to obtain up to 1 mA tube current per pixel. Activation and modulation of the x-ray radiation were achieved by programming the input voltage pulse train applied to the gate of the metal-oxide-semiconductor field effect transistor (MOSFET) circuit connected to the cathode [Fig. 1(b)], which served as a toggle switch.

[a)]Electronic mail: zhou@physics.unc.edu

 

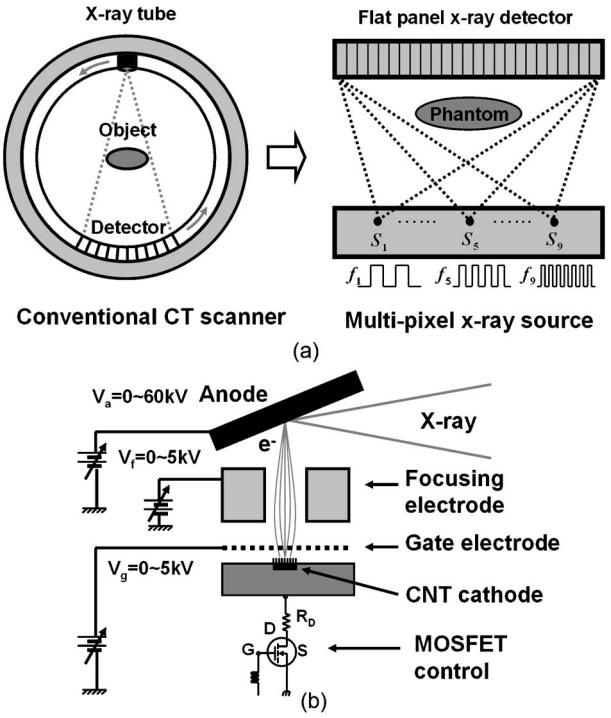


FIG. 1. (a) Schematics of the conventional CT scanner (left) and the multiplexing imaging system using a nine-pixel x-ray source and a digital area detector (right). (b) Each individual x-ray pixel of the multipixel x-ray source is comprised of a CNT based field emission cathode, a 150 $\mu$m thick dielectric spacer, an extraction gate, and a focusing electrode. The cathode was a thin CNT composite film deposited on a metal substrate by electrophoresis.

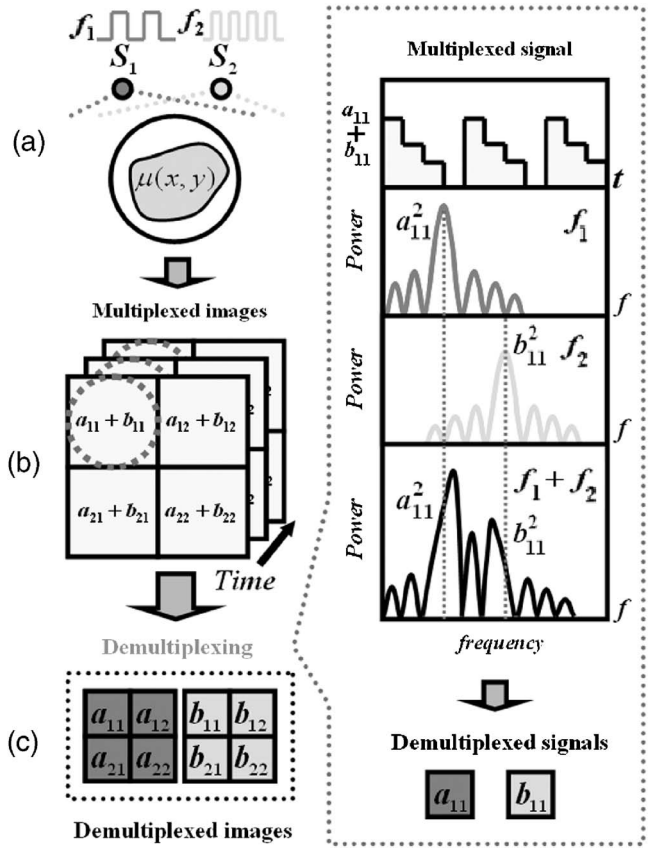


FIG. 2. The flow chart for the OFDM imaging process. (a) Two incident x-ray beams with the respective pulsing frequencies of $f_1$ and $f_2$ transmitted through the phantom and formed a multiplexed x-ray signal including both frequency components. (b) The multiplexed images were recorded by a single flat panel x-ray detector which collected the transmitted x-ray intensity as a function of time over a certain period $T$. (c) DFT algorithm was used to demultiplex the composite x-ray signals recorded by a detector pixel. The orthogonal nature of the signals was a result of the peak of each subcarrier corresponding to the nulls of other subcarriers. (d) The demultiplexed images were achieved by repeating the demultiplexing procedure for all the detector pixels.

A computer circuit board was imaged using the nine-pixel x-ray source operating in the cone-beam geometry with a flat panel detector running at 16 fps. The imaging and data processing procedures are illustrated by the flow chart in Fig. 2. All the x-ray pixels were activated *simultaneously* for 10 s, as illustrated in Fig. 3(a). Each x-ray beam had a square wave form, 50% duty cycle, and a unique frequency $f_i$ ($i=1-9$). Although sampling at twice the Nyquist frequency can ensure the correct measurement of $f$, the detector frame rate ($f_d$) needs to be sufficiently faster than the highest pulsing frequency $f_{\max}$ to obtain the correct wave form. In the present experiment, $f_d > 10\, f_{\max}$. Overlapping intensity contributions from the primary and higher harmonics of the input signals and their ripples in the Fourier spectrum introduce imaging artifacts due to interchannel interferences. These were eliminated by setting the bandwidth $\Delta f < 2f_{\min}$ (the second order harmonic is zero for 50% duty square wave) and by using nine *orthogonal* frequencies[12] in the range 0.5 and 1.3 Hz with an interval of 0.1 Hz, as shown in Fig. 3(b).

The transmitted x-ray intensities ($I$) were recorded as a function of time ($t$). Due to the large number of overlapping wave forms, the $I$ vs. $t$ data of each detector pixel, shown in Fig. 3(c), appear to be random. Figure 3(d) shows one frame of the multiplexed images, which, as a superposition of projections from different angles, shows no apparent information of the object being imaged, as expected. Although structures were observed in the corresponding power spectrum from discrete Fourier transform (DFT) [Fig. 4(a)], the peak positions were not related to the frequencies of the input signals. It can be shown that, $I^i_{jk} = \alpha \sqrt{I_{jk}|_{f=f_i}}$, where $I^i_{jk}$ is the signal from the $i$th x-ray beam recorded on the $jk$th detector pixel, $I_{jk}|_{f=f_i}$ is the intensity at one of the nine orthogonal frequencies $f_i$ ($i=1-9$) in the power spectrum, and $\alpha$ is a constant. By demultiplexing the x-ray signals pixel by pixel across the entire detector, clear projection images of the object from the nine viewing angles were extracted and are shown in Fig. 4(b).

To assess the quality of the images obtained by multiplexing, a demultiplexed image $S_1$ [Fig. 4(c)] was compared to a reference image $S_1{}^o$ [Fig. 4(d)], which was taken using the same x-ray pixel under the same imaging conditions (kilovolts, milliamperes, time, and geometry) without using multiplexing/demultiplexing. The two images appear to have the same contrast and spatial resolution. No visual difference was detected. More quantitative analysis showed that the intensity deviation between the two sets of data was found to be less than 3%. This difference is attributed to the intensity fluctuation of the x-ray beam which is estimated to be around 1%, drifting of the detector sampling rate (around 0.1 fps) and insufficient data sampling due to the limitation of the x-ray detector. Separate simulation has shown the improvement of the image quality with increased detector sampling rate.

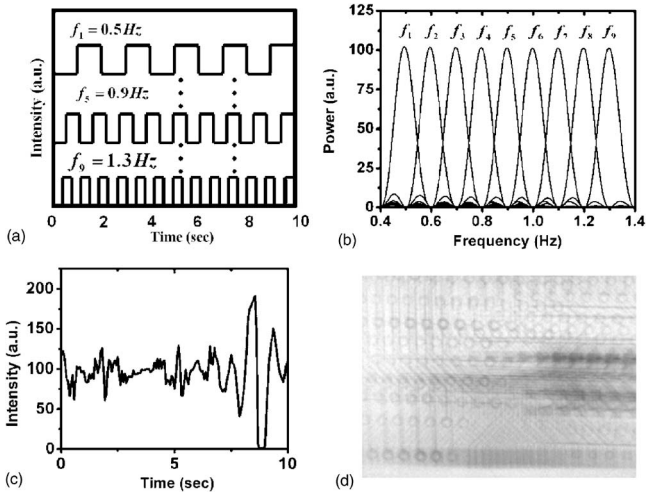


FIG. 3. (a) A schematic showing the wave forms used for the nine x-ray beams in this experiment. The pulsing frequencies ranged from 0.5 to 1.3 Hz with 0.1 Hz frequency separation. (b) In frequency domain, the simulation demonstrated that, at the central frequency of each subcarrier, there was no cross-talk from the other subcarriers due to the orthogonality of the signals. (c) The transmitted x-ray intensity vs time data recorded on one detector pixel. (d) One frame of a typical multiplexed x-ray image of the computer board.

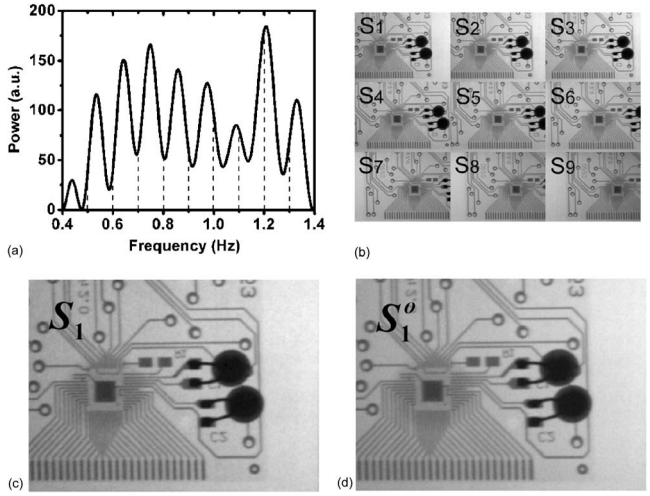


FIG. 4. (a) The DFT based algorithm was applied to demultiplex the multiplexing x-ray signal showed in Fig. 3(d). (b) Nine demultiplexed images corresponding to nine frequency channels were obtained by the OFDM scheme showing the circuit board from different viewing angles. (c) One of the demultiplexed images of the circuit board from the x-ray pixel $S_1$. (d) A projection image taken using only the x-ray pixel $S_1$ with the same dose and geometry as in (c). The difference between the two images is visually negligible.

Compared with sequential imaging, multiplexing generates more scattered photons because multiple x-ray beams illuminate the sample simultaneously. The contribution of the scattered photons from different x-ray beams, however, can be separated in the demultiplexing process because they have the same modulation frequencies as their corresponding primary beams. As a result, the additional scattering intensity does not contribute to the noise level in the demultiplexed image. In practice, however, the use of multiplexing requires redesign the antiscattering grid which is commonly and effectively used in medical imaging systems.

The multiplexing imaging speed in this study is limited by the maximum frame rate of the *area* detectors which are usually less than 50 fps. Overall the experiment has sufficiently demonstrated the efficiency of multiplexing for data collection compared to the current serial approach. In the present experiment using the OFDM scheme the imaging time for the nine projections was 10 s. If taken sequentially one at a time the same images would require a total of 45 s with the same x-ray peak power at 100% duty cycle (5 s per image for the same x-ray dose). In general a factor of $N/2$ ($N$=total number of images) increase in the speed can be achieved using the OFDM scheme. This becomes significant when $N$ is large, for example, for clinical CT scanners which use $\sim$1000 views per gantry rotation.[10] On the other hand, if the total imaging time and x-ray dose are kept the same as used in the *sequential* process, then the x-ray peak power, i.e., the tube peak current, can be reduced by a factor of $N/2$ by multiplexing because the exposure time per image is now longer.

This work was partially supported by NIH-NIBIB (4R33EB004204-01), NIH-NCI (U54CA119343), TSA (Manhattan II), and Xintek, Inc. The authors acknowledge helpful discussion with D. Lalush.

[1] G. N. Hounsfield, Br. J. Radiol. **46**, 1016 (1973).
[2] A. M. Cormack, Phys. Med. Biol. **18**, 195 (1973).
[3] J. Hsieh, *Computed Tomography: Principles, Design, Artifacts, and Recent Advances* (SPIE, Bellingham, WA, 2003).
[4] J. T. Dobbins and D. J. Godfrey, Phys. Med. Biol. **48**, R65 (2003).
[5] T. D. Moore, D. Vanderstraeten, and P. M. Forssell, IEEE Trans. Compon. Packag. Technol. **25**, 224 (2002).
[6] M. J. Paulus, S. S. Gleason, S. J. Kennel, P. R. Hunsickler, and D. K. Johnson, Neoplasia **2**, 62 (2000).
[7] F. Kiessling, S. Greschus, M. P. Lichy, M. Bock, C. Fink, S. Vosseler, J. Moll, M. M. Mueller, N. E. Fusenig, H. Traupe, and W. Semmler, Nat. Med. **10**, 1133 (2004).
[8] B. Ohnesorge and T. Flohr, Electromedica **68**, 1 (2000).
[9] J. J. Froelich and H. J. Wagner, Cardiovasc. Intervent Radiol. **24**, 297 (2001).
[10] A. B. Wolbarst and W. R. Hendee, Radiology **238**, 16 (2006).
[11] P. Schardt, J. Deuringer, J. Freudenberger, E. Hell, W. Knupfer, D. Mattern, and M. Schild, Med. Phys. **31**, 2699 (2004).
[12] A. V. Oppenheim, A. S. Willsky, and I. T. Young, *Signals and Systems* (Prentice-Hall, Englewood Cliffs, NJ, 1983).
[13] P. J. Treado and M. D. Morris, Anal. Chem. **61**, 732A (1989).
[14] R. N. Zare, F. M. Fernandez, and J. R. Kimmel, Angew. Chem., Int. Ed. Engl. **42**, 30 (2003).
[15] O. Zhou, J. P. Lu, and Q. Qiu, U.S. Patent No. 6,876,724 (5, April 2005).
[16] J. Zhang, G. Yang, Y. Cheng, B. Gao, Q. Qiu, Y. Z. Lee, J. P. Lu, and O. Zhou, Appl. Phys. Lett. **86**, 184104 (2005).
[17] M. S. Dresselhaus, G. Dresselhaus, and P. Avouris, *Carbon Nanotubes: Synthesis, Structure, Properties and Applications*, Topics in Applied Physics Vol. 80 (Springer, Heidelberg, 2000).
[18] Y. Cheng, J. Zhang, Y. Z. Lee, B. Gao, S. Dike, W. L. Lin, J. P. Lu, and O. Zhou, Rev. Sci. Instrum. **75**, 3264 (2004).
[19] R. W. Chang, Bell Syst. Tech. J. **46**, 1775 (1966).
[20] I. Brodie and C. A. Spindt, Adv. Electron. Electron Phys. **83**, 1 (1992).
[21] J. Zhang, Y. Cheng, Y. Z. Lee, B. Gao, Q. Qiu, W. L. Lin, D. Lalush, J. P. Lu, and O. Zhou, Rev. Sci. Instrum. **76**, 094301 (2005).